INTERNATIONAL
Agrophysics
www.international-agrophysics.org

Int. Agrophys., 2023, 37, 141-149
doi: 10.31545/intagr/161612

Physical and thermal modification of selected lignocellulosic raw materials

Karol Kupryaniuk[1]*, *Tomasz Oniszczuk*[1]*, *Maciej Combrzyński*[1], *Arkadiusz Matwijczuk*[2,3], *and Jakub Pulka*[4]

[1]Department of Thermal Technology and Food Process Engineering, University of Life Sciences in Lublin, Głęboka 31, 20-612 Lublin, Poland
[2]Department of Biophysics, University of Life Sciences in Lublin, Akademicka 13, 20-950 Lublin, Poland
[3]ECOTECH-COMPLEX-Analytical and Programme Centre for Advanced Environmentally-Friendly Technologies, Maria Curie-Skłodowska University, Głęboka 39, 20-033 Lublin, Poland
[4]Department of Biosystems Engineering, University of Life Sciences in Poznań, Wojska Polskiego 50, 60-627 Poznań, Poland

Received January 26, 2023; accepted February 24, 2023

A b s t r a c t. The impact of the modification of the plasticizing system of the TS-45 single-screw extruder (by ZMCh Metalchem, Gliwice, Poland) with L/D = 12 is discussed in the article. The modification involved the reconfiguration of the extruder screw to achieve certain selected physical characteristics of the lignocellulosic raw materials which are not commonly used in biogas facilities. Shredded lignocellulosic raw materials (corn straw, wheat straw, and hay) were moistened to achieve a 25% water content and extruded at three rotational speeds of the extruder screw: 70, 90, and 110 rpm. During extrusion-cooking, the process efficiency and energy intensity were determined. The obtained extrudates were studied in order to establish selected physical properties (water solubility index, water absorption index and bulk density). In addition, the research included an analysis of microscopic images and the efficiency of cumulative methane and biogas production per fresh mass, dry mass, and dry organic mass. In addition, an analysis of the FTIR infrared spectra of the studied extruded samples was performed, these contained lignocellulose structures, and revealed explicit changes at the molecular level. The use of the extrusion technique as a pretreatment of the plant biomass allowed for the lignocellulosic bonds to be broken, which loosened the structure of the material and thus changed its physical properties and biogas efficiency.

K e y w o r d s: pretreatment, lignocellulosic biomass, mechanical properties, extrusion-cooking process, FTIR spectroscopy

INTRODUCTION

The current geopolitical situation, the growing awareness of whole societies regarding environmental issues and rising electricity prices have all contributed to the dynamic development of the power industry. In particular, the use of biogas in power generation is gaining in importance (Zając *et al.,* 2017). Many research centres in Poland and abroad are exploring the possibilities of raising the efficiency level of the methane fermentation process in agricultural biogas plants. Agricultural biomass is among the primary sources of substrates used in biogas facilities. The biomass material contains annual and perennial energy crops, agricultural residues (straw, stems, corn cobs, *etc.*), and by-products of the food industry (from the dairy, sugar, distilling industries, *etc.*). Lignocellulosic biomass in the form of cereal straw, in particular wheat straw, which contains cellulose, lignins, and hemicellulose, is also used in the production of bioethanol after being pretreated by hydrolysis (Perea-Moreno *et al.,* 2019; Marks-Bielska *et al.,* 2019). In recent years, there has been an increase in the quantity of corn crops grown for grain in Poland. Corn straw is a common agricultural waste that is often disposed of inappropriately (*e.g.* incineration, tillage). As a consequence, lignocellulosic

*Corresponding author e-mail: tomasz.oniszczuk@up.lublin.pl
karol.kupryaniuk@o2.pl

© 2023 Institute of Agrophysics, Polish Academy of Sciences

biomass that could otherwise be utilized in agricultural biogas facilities is lost (Li *et al.,* 2018). In order to be used in a biogas plant, straw must undergo pretreatment which involves a physical and thermal process that severs the lignocellulosic bonds. The pretreatment of lignocellulosic biomass facilitates the improved mixing and sinking of the charge in the digester chamber, which enhances the efficiency of the plant. The extrusion-cooking technique, which is well-known from the food sector (Mitrus *et al.,* 2020), was proposed for the pretreatment. It is used to break lignocellulosic bonds and has a positive effect on methane fermentation (Zhang *et al.,* 2021; Zheng and Rehmann, 2014; Vandenbossche *et al*., 2014; Liu *et al.,* 2022). Moreover, the extrusion-cooking process is capable of accelerating the decomposition of lignocellulosic biomass by thermophilic bacteria; it also improves both substrate solubility and bioavailability (Wang *et al.,* 2022).

The aim of the research was to determine the effect of pretreatment on the physical and chemical properties and biogas efficiency of the lignocellulosic raw materials used in biogas plants. The study also relied on FTIR spectroscopy measurements (Fourier Transform Infrared Spectroscopy) to determine changes in the tested samples occurring at a molecular level during the extrusion-cooking process.

MATERIALS AND METHODS

The following lignocellulosic raw materials were used in the research project: corn straw, hay, and wheat straw obtained from Radosław Sebastianiuk's farm (Mokrany Nowe, Poland). Such materials are not commonly used in biogas facilities. The raw materials were shredded using an CF420B hammer mill (Pavolt, Zrębice, Poland) to achieve a fraction size of 5 to 10 mm. Next, they were moistened to form a mixture with a 25% water content and sealed tightly in plastic bags to reduce water migration and also achieve homogenization. The prepared samples were placed in ambient conditions in a laboratory. After 24 h, the moistened samples were mixed again and subjected to the extrusion-cooking process at three different rotational speeds of the extruder screw (70, 90, and 110 rpm). A TS-45 single-screw extruder (Metalchem, Gliwice, Poland) was used, it was equipped with a modified plasticizing system with an L/D = 12 ratio. The screw was equipped with an additional section of beaters to ensure the improved compaction of the processed raw material before its moulding phase at the extruder head. The temperature ranges during the process were the following: from 70 to 110°C for section 1, from 131 to 166°C for section 2, and from 68 to 123°C for the extruder head. After the extrusion-cooking process, the obtained extrudates were dried in a laboratory dryer.

The process efficiency was expressed in terms of the output of the extruder and was measured by determining the mass of the extrudate obtained in a specific time for all the raw materials and processing conditions used (Matysiak *et al.,* 2018).

Energy consumption, expressed as specific mechanical energy (SME) was calculated by taking into account the engine load, the extruder working parameters and process efficiency (Combrzyński *et al.,* 2020).

The bulk density was measured by weighing the mass of the specific volume of the tested material (Lisiecka *et al.,* 2021a).

The water absorption index (WAI) and the water solubility index (WSI) were used to evaluate the treatment intensity of the extrusion-cooking method applied, as described by Bouasla *et al.* (2016) and Lisiecka *et al.* (2021b).

A stereoscopic ZEISS Stemi 508 Greenough with an 8:1 zoom (Carl Zeiss, Poznań, Poland) microscope was used to take the pictures. The structure was analysed using a microscope with a magnification of ×1.0 and an external light source (Combrzyński *et al*., 2022). Photos were taken of the control sample (untreated) and also of the extruded materials.

Using FTIR spectroscopy, spectra were obtained with an IRSpirit spectrometer by Shimatzu (Japan). An ATR (Attenuated Total Reflection) accessory was used. It was a ZnSe crystal with a strictly defined geometry (*i.e.* truncated at 45°). It offers a 20-fold internal reflection of an absorbed beam, thus significantly increasing the signal strength. During the measurement, 24 scans were recorded for each sample. Next, the program averaged the results for all of the collected spectra. Before each measurement, the crystal was thoroughly cleaned using ultra-pure solvents acquired from Sigma-Aldrich (Saint Louis, Missouri, USA). For about 1 h before and during the measurement, an atmosphere of inert gas N_2 was maintained in the measuring cell. The spectra measurements were recorded across the range from 450 to 3 750 cm^{-1} at a resolution of 2 cm^{-1}. The measurements were performed in the Laboratory of the Department of Biophysics, in the University of Life Sciences in Lublin. At the final stage, the spectra were analysed and processed using Grams/AI software supplied by Thermo Galactic Industries (Waltham, USA). All of the spectra were measured at ambient temperature (Sadowska *et al.,* 2019).

The biogas efficiency measurement was conducted at the Laboratory of Ecotechnologies, University of Life Sciences in Poznań. The efficiency of the methane fermentation process was investigated under mesophilic conditions (the most common technology in Europe) in three replications with the use of proprietary biofermentors (Cieślik *et al*., 2016). The samples pretreated with extrusion-cooking were analysed for biogas production efficiency in accordance with the generally recognized standards: DIN 38414/S8 and VDI 4630 (Kowalczyk-Juśko *et al*., 2017). The biogas yield was measured (m^3 Mg^{-1}) relative to the fresh mass, dry mass, and dry organic mass, as described by Dach *et al*. (2014).

The results were analysed using Statistica 13.3 software (StatSoft, Kraków, Poland) in order to investigate the effect of the rotational speed of the extruder screw on the obtained results. Pearson's correlation coefficients were assessed, and an analysis of variance was performed at a confidence level of 95% ($\alpha = 0.05$). In addition, Tukey's test was used to compare pairs of means.

RESULTS AND DISCUSSION

The parameters of the extrusion-cooking process were recorded on production sheets, depending on the raw materials used and the screw rotation speed. As shown in Table 1, the processing efficiency determined during the extrusion-cooking process was significantly higher if the wheat straw was processed at extruder screw speeds of 70 and 90 rpm.

The highest level of efficiency of the process (15.20 kg h^{-1}) was seen in samples of wheat straw extruded at a screw speed of 90 rpm. For corn straw and hay, the highest values of the tested parameter were 13.56 and 13.12 kg h^{-1}, respectively. The lowest efficiency values were reported when using the lowest screw speed. For corn straw, wheat straw and hay, the lowest recorded efficiency measurements were: 5.12, 10.08 and 7.92 kg h^{-1}. The lowest output values for corn straw may be explained by the highest index of mechanical strength for the raw material (Niedziółka *et al.,* 2012). For this raw material, the extent of the shearing forces should probably be increased, *e.g*. by increasing the screw speed. This theory was confirmed by the measurement results. Kupryaniuk *et al.* (2019, 2020a) demonstrated this when the standard plasticizing system of the TS-45 single-screw extruder was applied and a lower efficiency in the extrusion-cooking of the corn straw and wheat straw was observed. Presumably, the modification of the plasticizing system through the use of a retracting and mixing zone at the final section of the extruder screw permits the compaction, retraction, and deaeration of the processed raw material.

Another parameter of the extrusion-cooking process that was tested was its energy consumption intensity. The highest SME value (0.581 kWh kg^{-1}) was recorded for corn straw subjected to extrusion-cooking at the lowest rotational speed of the screw. For hay and wheat straw, the values were: 0.518 and 0.499 kWh kg^{-1} (110 rpm), respectively. The lowest SME value (0.257 kWh kg^{-1}) was measured when wheat straw was extruded at a screw speed of 90 rpm. For corn straw and hay, the values were: 0.501 kWh kg^{-1} (110 rpm) and 0.359 kWh kg^{-1} (70 rpm), respectively. In the cases of corn and wheat straws, the factor decreased as compared to the tests carried out previously using a standard plasticizing system (Kupryaniuk *et al.* 2019, 2020a, 2020b).

The extrudates obtained were tested for selected physical properties. The influence of mechanical and thermal treatment on the changes in the physical properties of these raw materials and their biogas efficiency was established.

The bulk density of the raw materials was determined before and after the extrusion-cooking process was completed. For the control samples without treatment, the bulk densities were found to be: 72.94 kg m^{-3} (corn straw), 90.65 kg m^{-3} (wheat straw), and 138.08 kg m^{-3} (hay), respectively. Corn straw was the only exception as the control sample did not show a higher value of bulk density after pretreatment. The extrusion-cooking process was observed to have caused the breaking of the lignocellulosic bonds, which resulted in much lower bulk densities of wheat straw and hay. In the case of the extruded samples, the lowest values were: 66.94 kg m^{-3} (corn straw, 90 rpm), 58.05 kg m^{-3} (wheat straw, 70 rpm), and 96.08 kg m^{-3} (hay, 90 rpm). The high bulk density measurements were: 87.05 kg m^{-3} (corn straw, 110 rpm), 69.79 kg m^{-3} (wheat straw, 90 rpm), and

Table 1. Results of the extrusion-cooking processing conditions and selected physical properties of the lignocellulosic raw materials

Sample	SS (rpm)	Q (kg h^{-1})	SME (kWh kg^{-1})	BD (kg m^{-3})	WAI (g g^{-1})	WSI (%)
Corn straw	Control	-	-	72.94^{b}	9.75^{d}	4.99^{a}
	70	5.12^{a}	0.581^{a}	77.21^{c}	5.81^{b}	9.80^{b}
	90	8.48^{b}	0.487^{a}	66.94^{a}	6.12^{c}	10.85^{c}
	110	13.56^{c}	0.501^{a}	87.05^{d}	5.57^{a}	9.94^{b}
Wheat straw	Control	-	-	90.65^{d}	7.88^{b}	8.77^{a}
	70	10.08^{a}	0.268^{a}	58.05^{a}	5.68^{a}	14.02^{c}
	90	15.20^{c}	0.257^{a}	69.79^{c}	6.36^{a}	12.02^{b}
	110	13.44^{b}	0.499^{b}	65.38^{b}	6.18^{a}	14.35^{c}
Hay	Control	-	-	138.08^{d}	6.08^{b}	15.72^{d}
	70	7.92^{a}	0.359^{a}	106.18^{c}	3.82^{a}	11.26^{a}
	90	9.12^{b}	0.463^{b}	96.08^{a}	4.30^{a}	13.86^{c}
	110	13.12^{c}	0.518^{b}	98.11^{b}	4.04^{a}	12.45^{b}

SS – screw speed, Q – efficiency, SME – specific mechanical energy, BD – bulk density, WAI – water absorption index, WSI – water solubility index, $^{a-d}$ refers to individual variables.

106.18 (hay, 70 rpm). These results are lower than those reported by Victorin *et al*. (2020), who had used a twin-screw extruder. They obtained a density value of wheat straw of 334 kg m^{-3} .

The influence of extrusion-cooking on the capacity of the obtained extrudates to absorb water (WAI) was determined. As shown in Table 1, in each case the control sample was characterized by the highest WAI value as compared to the same index value reported for samples subjected to the extrusion-cooking pretreatment. For corn straw extrudates, the highest WAI (6.12 g g^{-1}) was seen in a sample extruded at the screw speed of 90 rpm. The lowest WAI value (5.57 g g^{-1}) was reported at the highest speeds. For both wheat straw and hay, the lowest WAI values (5.68 and 3.82 g g^{-1}, respectively) were recorded for samples extruded at the lowest rotational speed of the extruder screw. For the same tested raw materials, the highest WAI values were 6.36 g g^{-1} (wheat straw, 90 rpm) and 4.04 (hay, 90 rpm). The lower WAI value coincided with higher BD results. As regards hay, this dependence was observed across the entire range of screw speeds, including the control sample. The results achieved were confirmed by an analysis of the microstructure and infrared spectra. When a standard plasticizing system was used, only the hay samples were reported to demonstrate lower WAI values. In the case of corn straw and wheat straw, the use of a modified plasticizing system increased the WAI values (Kupryaniuk *et al*., 2019, 2020b).

Along with WAI measurements, the solubility of the raw material in water was also tested (WSI). Obtaining the WSI value may enhance the operation of a biogas plant by ensuring a more intense mixing of the charge and a higher biogas yield (Kupryaniuk *et al.*, 2022). Only in the case of hay were lower measurements recorded as compared to the control sample. For the corn straw and hay extrudates, the highest WSI values were obtained for samples extruded at a screw speed of 90 rpm (10.85 and 13.86%, respectively), and for wheat straw (14.35%), the highest value was recorded for a sample processed using the highest screw speed. In the case of corn straw (4.99%) and hay (11.26%), the lowest WSI values were reported in samples extruded at the lowest screw speeds. In the case of wheat straw extrudates (12.02%), the lowest value was observed in samples extruded at a speed of 90 rpm. The use of a modified plasticizing system raised the WSI value across the entire range of screw speeds that were applied to each of the tested raw materials in relation to the control samples. During the extrusion-cooking process using the standard plasticizing system, the highest WSI values achieved were: 2.85% (corn straw, 70 rpm), 4.85% (wheat straw, 110 rpm) and 10.38% (hay, 70 rpm), and the lowest were: 2.42% (corn straw, 110 rpm), 3.52% (wheat straw, 70 rpm), and 9.89% (hay, 110 rpm) (Kupryaniuk *et al.,* 2019, 2020b).

Microscopic images were used to determine the degree of degradation of lignocellulosic bonds according to the extrusion-cooking conditions. The images of the individual raw materials are shown below, starting with those not subjected to the extrusion-cooking pretreatment and finishing with those extruded at rising rotational speeds of the extruder screw. Unextruded corn straw is characterized by the clusters of unprocessed starch surrounding it (Fig. 1A). Extrusion-cooking disintegrated these clusters, and the shear forces in the extruder cylinder destroyed the structure of the material. The starch clusters were reduced as the rotational speed increased. The application of the highest screw speed (Fig. 1D) facilitated the agglomeration of the material, which was demonstrated by the bulk density measurements.

The microscopic images of wheat straw, as was the case with corn straw, prove that extrusion-cooking altered the structure of the material (Fig. 2). The starch clusters also disintegrated in this material (Fig. 1B-1D). However in the case of corn straw, the use of a screw speed of 90 rpm allowed for the production of extrudates with the greatest material agglomeration and the highest density among all of the extruded materials.

In the case of hay (Fig. 3), as is the case with the other raw materials studied, the structure of the material changed, and the starch clusters were broken. Unlike in the case of corn (Fig. 1) and wheat straws (Fig. 2), the application of a screw speed of 70 rpm (Fig. 3B) resulted in the highest degree of material agglomeration, which was observed in bulk density measurements.

In order to reveal the changes occurring at a molecular level, infrared spectroscopy was used. It helps to determine the impact of the extrusion-cooking process on transformations occurring in individual raw materials. Figure 4 shows the spectra for corn (for wheat and hay, comparable results are presented in Table 2). On the other hand, in Table 2

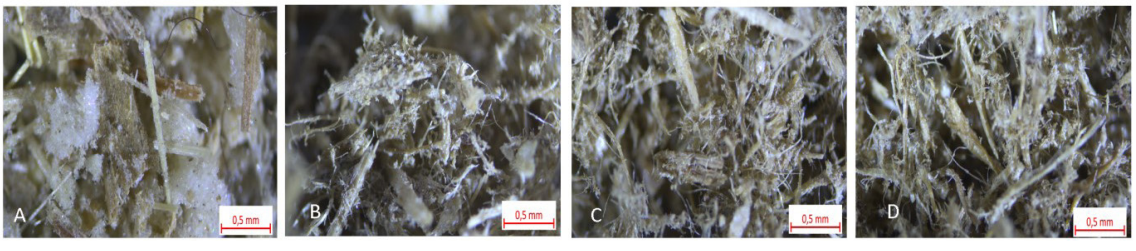

Fig. 1. Microscopic images of corn straw: A – control sample; and samples extruded at: B – 70 rpm, C – 90 rpm, and D – 110 rpm.

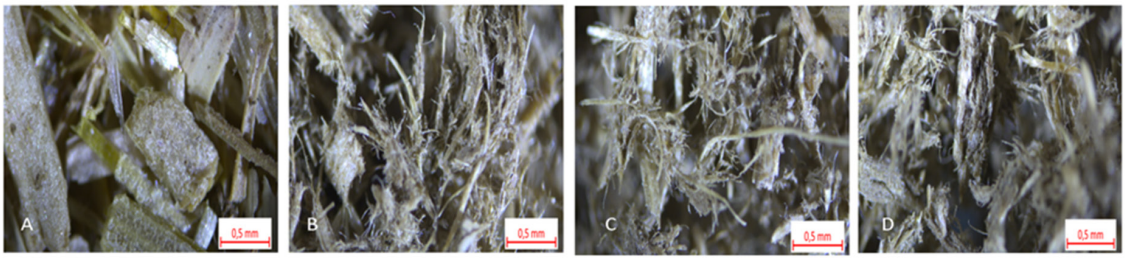

Fig. 2. Microscopic images of wheat straw: A – control sample; and samples extruded at: B – 70 rpm, C – 90 rpm, and D – 110 rpm.

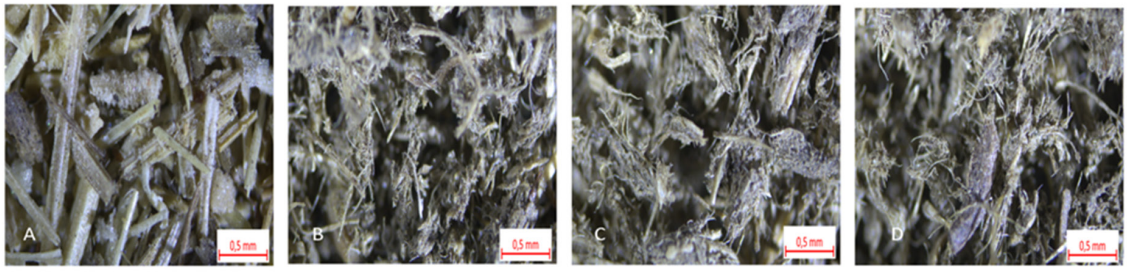

Fig. 3. Microscopic images of lignified hay: A – control sample; and samples extruded at: B – 70 rpm, C – 90 rpm, and D – 110 rpm.

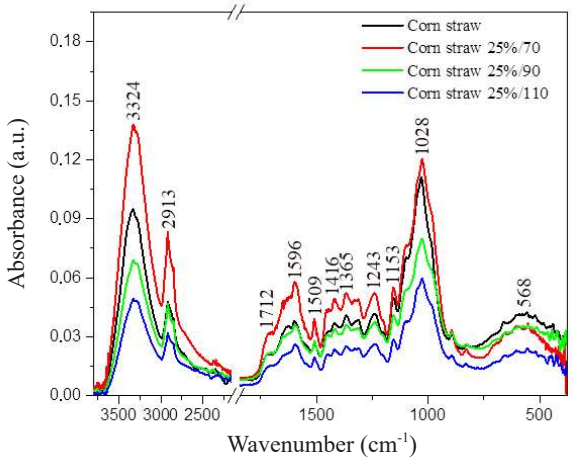

Fig. 4. FTIR spectra for the analysed samples measured in the spectral range from 800 to 3 200 cm^{-1}. The spectra were measured at ambient temperature.

(also for wheat and hay), relevant bands were assigned to the vibrations of the characteristic functional groups occurring in samples containing lignocellulosic structures.

When characterizing the most significant vibrations in the obtained FTIR spectra, the highest wave numbers should be given priority. According to Xu *et al.* (2015), Ong *et al.* (2021) and others, a vibration area with a maximum of ~3 330 cm^{-1} corresponds to the stretching vibrations of hydroxyl groups found in the structure of lignocellulose. Evidently, the intensity of these vibrations mainly depends on the screw speed (rpm) during the extrusion-cooking process. This area mainly shows changes in intensity related to the formation of intermolecular hydrogen bonds. By contrast, the area with a sharp maximum peak at approximately 2 910 cm^{-1} corresponds to the stretching vibrations of the C-H groups in the CH_2 and CH_3 groups found in the lignocellulosic structures (Kupryaniuk *et al.,* 2020a, b; Combrzyński *et al*., 2022; Zhang *et al*., 2020).

Vibrations with a peak occurring at approximately 1 715 cm^{-1} correspond to the stretching vibrations of the carbonyl group C=O (Zhuang *et al*., 2020; Fei *et al*., 2020). Other relevant areas of vibrations with a peak at ~1 640, 1 600 or 1 510 cm^{-1} are characteristic of the deformation vibrations of –OH groups (Xu *et al*., 2015; Asadieraghi *et al*., 2014). Typically, in samples containing mainly lignocellulosic structures and their derivatives, this area primarily typifies the stretching vibrations of C=C groups (Varma *et al*., 2017; Zhang *et al.,* 2020). Apart from a significant and reliable change in intensity, this area also shows a minor change in proportion between the 1 644 and 1 596 cm^{-1} peaks after extrusion-cooking, which also confirms their micronization through degradation changes in the bonds of the lignocellulose structure, which, ultimately, considerably facilitates their fermentation.

This effect is visible in the samples selected for testing (*e.g.* Fig. 4). These changes may therefore serve as a positive molecular marker of changes occurring in the structure of lignocellulose during various conditions of the extrusion-cooking process. Next, there are very characteristic bands in the spectra with peaks of, for example, ~1 450, 1 416, 1 365 or 1 243 cm^{-1} (in Fig. 4, slightly shifted in wheat and hay – as shown in Table 2). They correspond primarily to the deformation vibrations of the CH group in the $–CH_2$ structures found in lignocellulose (Ong *et al*., 2021; Gabhane *et al.,* 2015). Another vibration area with a wide peak at ~1 030 cm^{-1} belongs to the stretching vibrations in the C-O groups typical of cellulose and, as a consequence,

Table 2. Locations of FTIR absorption band maxima and the assignment of particular vibrations to the respective samples: corn straw, wheat straw and hay

FTIR			Type and origin of vibrations
Band location (cm^{-1})			
Corn straw	Wheat straw	Hay	
3 324	3 333	3 324	ν(O-H) in H_2O and intramolecular hydrogen bonding
2 913	2 913	2 913	ν(C-H) in CH_2 and CH_3 asymmetrical and symmetrical
2 843	2 844	2 852	
1 712	1 725	1 719	ν(C=O) or carboxyl group
1 644	1 641	1 637	
1 596	1 591	1 596	ν(C=C) and δ(O-H) in adsorbed H_2O
1 509	1 503	1 509	
1 453	1 458	1 446	
1 416	1 416	1 416	δ(-OH in plane), δ(CH_2), δ(C-H) and ν(COO^-)
1 365	1 365	1 365	
1 308	1 313	1 316	
1 243	1 233	1 236	δ(C-H) and antisymmetric bridge oxygen stretching –OH in-plane bending
1 199	1 194	1 197	δ(C-H) and ν(C-O)
1 153	1 156	1 156	
1 106	1 104	1 093	antisymmetric in phase ring stretching and ν(C-O-C) and ring stretching modes
1 028	1 031	1 024	
975	974	985	
893	893	890	CH_2 rocking β-linkage of cellulose ring breathing and antisymmetric out of phase stretching -OH out-of-plane bending and CH_2 rocking
825	827	833	
568	552	520	

ν – stretching vibrations, δ – deformation vibrations, s – symmetric, as – asymmetric, st – strong, w – weak.

to the lignocellulosic structures (Combrzyński *et al.,* 2022; Asadieraghi *et al*., 2014), and also, above all, in the vibration system of the C-O-C group which takes part in the formation of characteristic bonds between the structural units of lignocellulose. A notable decrease in the intensity of vibrations in this area confirms the breaking of large lignocellulosic structures, thus facilitating further processes of sample degradation. Changes in the vibrations of the C-O-C groups were also linked to a notable difference in the intensity of vibrations below 900 cm^{-1}. The bands in this area are mainly, but not exclusively, associated with vibrations in the bonds of large fractions forming the structure of lignocellulose, namely in the α-1,6-glycosidic or α-1,4-glycosidic bonds (Zhang *et al*., 2008; Xu *et al.,* 2015). Evidently, the treatment factor applied to selected samples in FTIR spectroscopy tests also reveals their transformations at a molecular level.

The last stage of the research was to assess the effect of extrusion-cooking on the biogas efficiency of individual raw materials. Table 3 shows the obtained values.

The values obtained after the fermentation of the control samples (unextruded) were used for reference purposes. Samples of individual raw materials were considered in relation to fresh mass, dry mass, and dry organic mass, they were evaluated for their cumulative biogas and methane contents. For fresh mass determination, the lowest values were reported in the corn straw samples: 205.98 m^3 Mg^{-1} (110 rpm) for cumulative methane and 418.42 m^3 Mg^{-1} (70 rpm) for cumulative biogas. For cumulative methane, the highest value (219.70 m^3 Mg^{-1}) was recorded for wheat straw (110 rpm), which accounted for 11.42% of the methane yield (compared to the control sample). For cumulative biogas (375.56 m^3 Mg^{-1}), the highest value was recorded for hay (14.81%, 90 rpm). With regard to dry mass, the lowest values were recorded for corn straw, both for cumulative

Table 3. Biogas efficiency results of individual raw materials

Sample	Screw speed (rpm)	Methane content (%)	Cumulative production					
			Methane	Biogas	Methane	Biogas	Methane	Biogas
			(m^3 Mg^{-1} FM)		(m^3 Mg^{-1} DM)		(m^3 Mg^{-1} DOM)	
Corn straw	Control	50.97[b]	218.03[c]	427.78[c]	238.09[c]	467.13[c]	260.04[d]	510.20[c]
	70	49.39[a]	206.65[a]	418.42[a]	223.76[b]	453.03[b]	240.32[b]	486.55[a]
	90	49.23[a]	216.43[b]	439.58[d]	234.73[b]	476.75[d]	250.16[c]	508.10[b]
	110	48.83[a]	205.98[a]	421.79[b]	220.28[a]	451.08[a]	238.29[a]	487.97[a]
Wheat straw	Control	52.62[a]	197.18[a]	374.70[a]	222.95[a]	423.63[a]	243.16[a]	462.07[a]
	70	52.77[a]	213.19[b]	404.04[b]	231.96[b]	439.60[b]	255.26[b]	483.77[b]
	90	52.55[a]	213.72[b]	406.71[c]	232.40[b]	442.26[b]	256.51[b]	488.13[c]
	110	52.52[a]	219.70[c]	418.35[d]	236.56[c]	450.46[c]	260.92[c]	496.85[d]
Hay	Control	51.66[c]	168.97[a]	327.11[a]	182.83[b]	353.93[a]	215.76[c]	417.68[a]
	70	49.17[b]	168.41[a]	342.52[b]	181.38[a]	368.89[b]	212.42[a]	432.03[b]
	90	47.83[a]	179.62[b]	375.56[d]	193.81[c]	405.22[d]	225.38[c]	471.23[d]
	110	48.54[b]	168.67[a]	347.51[c]	182.88[b]	376.79[c]	214.29[b]	441.50[c]

FM – fresh mass, DM – dry mass, and DOM – dry organic mass. [a-d] refers to individual variables.

Table 4. Correlation matrix between processing variables, physical properties, and the biogas yield of the extrudates

	SS	Q	SME	BD	WAI	WSI	FM - CCH_4	FM - CB	DM - CCH_4	DM - CB	DOM - CCH_4
Q	0.738										
SME	0.390	-0.293									
BD	0.078	-0.137	0.249								
WAI	0.070	0.217	-0.090	-0.895							
WSI	0.138	-0.293	-0.352	-0.229	-0.080						
FM - CCH_4	0.042	0.171	-0.100	-0.928*	0.981*	-0.003					
FM - CB	0.096	0.022	0.155	-0.792	0.919*	-0.220	0.936*				
DM - CCH_4	0.017	0.163	-0.124	-0.943*	0.983*	0.010	0.999*	0.927*			
DM - CB	0.065	0.014	0.125	-0.820	0.930*	-0.203	0.943*	0.998*	0.938*		
DOM - CCH_4	0.043	0.268	-0.245	-0.957*	0.951*	0.210	0.971*	0.839	0.975*	0.854	
DOM - CB	0.138	0.086	0.095	-0.828	0.916*	-0.036	0.935*	0.975*	0.930*	0.978*	0.881

SS – screw speed, Q – efficiency, SME – specific mechanical energy, BD – bulk density, WAI – water absorption index, WSI – water solubility index, FM-CCH_4 – cumulative methane production (fresh mass), FM-CB – cumulative biogas production (fresh mass), DM-CCH_4 – cumulative methane production (dry mass), DM-CB – cumulative biogas production (dry mass), DOM-CCH_4 – cumulative methane production (dry organic mass), DOM-CB – cumulative biogas production (dry organic mass).

methane (220.28 m^3 Mg^{-1}, 110 rpm) and biogas (451.08 m^3 Mg^{-1}, 110 rpm). As was the case with fresh mass, the highest values were measured in the wheat straw samples (236.56 m^3 Mg^{-1}, 110 rpm) for cumulative methane (an increase of 6.10% as compared to the control sample) and hay 405.22 m^3 Mg^{-1} (14.49%, 90 rpm) for cumulative biogas. In terms of the dry organic mass, the lowest values of cumulative biogas and methane were observed in corn straw as compared to the control samples. For methane, the value was 238.29 m^3 Mg^{-1} (110 rpm) and a value of 486.55 m^3 Mg^{-1} (70 rpm) was determined in the case of biogas. The highest values for dry organic mass were measured in wheat straw. The methane yield achieved was 7.31% (260.92 m^3 Mg^{-1}, 110 rpm). In hay (471.23 m^3 Mg^{-1}, 90 rpm), the biogas yield was 12.82%. The application of a modified plasticizing system raised the yield of cumulative biogas in relation to fresh mass, dry mass, and dry organic mass.

Based on the measurements, a correlation matrix was designed to reflect the dependencies between the processing variables, the physical properties obtained, and the biogas yield (Table 4). The rotational speed was the factor observed to be the most closely correlated with efficiency. For the bulk density, there were clear correlations with cumulative methane production for all of the studied varia bles (fresh mass, dry mass, and dry organic mass). The WAI was closely correlated with both cumulative biogas

and cumulative methane production across the entire test range. For fresh mass and dry mass, cumulative methane production was closely correlated with all biogas yields. For fresh mass and dry mass, cumulative biogas production was not closely correlated with the remaining biogas yield for DOM-CCH_4 alone.

CONCLUSIONS

After performing the research described above, the following concluding remarks may be presented:

1. Variations in the rotational speed of the extruder screw apparently affected the measurements obtained. In the case of wheat straw, raising the screw speed to 90 rpm led to a significant increase in the efficiency of the process, thus producing the maximum measurement recorded. For the corn straw and wheat straw samples, a screw speed of 90 rpm reduced the energy requirements of the process.

2. Compared with the control sample, the application of extrusion-cooking led to a significant drop in water absorption index for all of the raw materials involved.

3. In the case of the water absorption index, only the unextruded hay sample returned significantly higher results compared to the extruded samples.

4. The measurements were supplemented by molecular tests carried out using FTIR spectroscopy. The bands observed may be used as markers of the spectroscopic changes occurring in processes related to the degradation of structures within the samples, including lignocellulosic ones, caused by the extrusion-cooking process. Band intensity variations were clearly observed, which may indicate the micronization of samples. The breakage of the bonds between the main structural units in lignocellulose was most evident from vibrations with peaks of *ca*. 3 330, 2 915, 1 600, 1 370, or 1 030 cm^{-1}.

5. In addition, a yield of cumulative biogas higher than that produced by the control samples was observed in all the raw materials used.

Conflict of interest: The authors declare that they have no known competing financial interests or personal relationships that could have appeared to influence the work reported in this paper.

REFERENCES

Asadieraghi M., and Daud W.M.A.W., 2014. Characterization of lignocellulosic biomass thermal degradation and physiochemical structure: Effects of demineralization by diverse acid solutions. Energy Convers. Manag., 82, 71-82. https://doi.org/10.1016/j.enconman.2014.03.007.

Bouasla A., Wójtowicz A., Zidoune M.N., Olech M., Nowak R., Mitrus M., and Oniszczuk A., 2016. Gluten-free precooked rice-yellow pea pasta: effect of extrusion-cooking conditions on phenolic acids composition, selected properties and microstructure. J. Food Sci., 81, C1070-C1079. https://doi.org/10.1111/1750-3841.13287.

Cieślik M., Dach J., Lewicki A., Smurzyńska A., Janczak D., Pawlicka-Kaczorowska J., Boniecki P., and Cyplik P., 2016. Methane fermentation of the maize straw silage under meso- and thermophilic conditions. Energy, 115(2), 1495-1502. https://doi.org/10.12911/22998993/76211.

Combrzyński M., Matwijczuk A., Wójtowicz A., Oniszczuk T., Karcz D., Szponar J., Niemczynowicz A., Bober D., Mitrus M., Kupryaniuk K., Stasiak M., Dobrzański B., and Oniszczuk A., 2020. Potato starch utilization in ecological loose-fill packaging materials-sustainability and characterization. Materials, 13, 1390. https://doi.org/10.3390/ma13061390.

Combrzyński M., Wójtowicz A., Oniszczuk A., Karcz D., Szponar J., and Matwijczuk AP., 2022. Selected physical and spectroscopic properties of TPS moldings enriched with durum wheat bran. Materials (Basel), 20, 15(14), 5061. https://doi:10.3390/ma15145061.

Dach J., Czekała W., Boniecki P., Lewicki A., and Piechota T., 2014. Specialised internet tool for biogas plant modelling and marked analysing. AMR, 909. 305-310. https://doi:10.4028/www.scientific.net/AMR.909.305.

Fei X., Jia W., Wang J., Chen T., and Ling Y., 2020. Study on enzymatic hydrolysis efficiency and physicochemical properties of cellulose and lignocellulose after pretreatment with electron beam irradiation. Int. J. Biol. Macromol., 145, 733-739. https://doi.org/10.1016/j.ijbiomac.2019.12.232.

Gabhane J., William S.P., Vaidya A.N., Das S., and Wate S.R., 2015. Solar assisted alkali pretreatment of garden biomass: Effects on lignocellulose degradation, enzymatic hydrolysis, crystallinity and ultra-structural changes in lignocellulose. Waste Manage., 40, 92-99. https://doi.org/10.1016/j.wasman.2015.03.002.

Kowalczyk-Juśko A., Kupryaniuk K., Oniszczuk T., Wójtowicz A., Janczak D., Smurzyńska A., Jóźwiakowski K., and Czechlowski M., 2017. Applicability of Jerusalem artichoke in agricultural biogas plants as maize silage alternative. Proc. 3rd Int. Conf. Energy Environment, University of Porto, Porto, Portugal. https://www.fep.up.pt/conferences/icee2017/images/ICEE2017_0808_VF.pdf.

Kupryaniuk K., Oniszczuk T., Combrzyński M., Dach J., and Czekała W., 2020a. Process efficiency and energy consumption during the extrusion of lignocellulosic materials. IOP Conference Series. Earth Environ. Sci., 505, 012040, 1-8. https://doi.org/10.1088/1755-1315/505/1/012040.

Kupryaniuk K., Oniszczuk T., Combrzyński M., Czekała W., and Matwijczuk A., 2020b. The influence of corn straw extrusion pretreatment parameters on methane fermentation performance. Materials, 13(13), 3003, 1-16. https://doi.org/10.3390/ma13133003

Kupryaniuk K., Oniszczuk T., Combrzyński M., Lisiecka K., and Janczak D., 2022. Influence of modification of the plasticizing system on the extrusion-cooking process and selected physicochemical properties of rapeseed and buckwheat straws. Materials, 15(14), 5039. https://doi.org/10.3390/ma15145039.

Kupryaniuk K., Oniszczuk T., Lisiecka K., and Kłapsia S., 2019. Impact of extrusion-cooking technique on lignocellulosic biomass. Badania i Rozwój Młodych Naukowców w Polsce. Uprawa roślin i ochrona środowiska. Młodzi Naukowcy, Poznań, 33-39. ISBN:978-83-66392-47-2.

Li W., Habiba K., Zhe Z., Zhang R., Liu G., Chang C., and Eva T., 2018. Methane production through anaerobic

digestion: Participation and digestion characteristics of cellulose, hemicellulose and lignin. Appl. Energy, 226, 1219-1228. https://doi.org/10.1016/j.apenergy.2018.05.055.

Lisiecka K., Wójtowicz A., and Gancarz M., 2021a. Characteristics of newly developed extruded products supplemented with plants in a form of microwave-expanded snacks. Materials (Basel), 14(11):2791. https://doi:10.3390/ma14112791.

Lisiecka K., Wójtowicz A., and Sujak A., 2021b. Effect of composition and processing conditions on selected properties of potato-based pellets and microwave-expanded snacks supplemented with fresh beetroot pulp. Pol. J. Food Nutr. Sci., 71(2), 211-236. https://doi.org/10.31883/pjfns/138321.

Liu Z., Jinzhi H., Yiqing Y., Mengyi W., and Li A., 2022. Effect of pretreatment by freeze vacuum drying on solid-state anaerobic digestion of corn straw. Fermentation, 8, 6, 259. https://doi.org/10.3390/fermentation8060259.

Marks-Bielska R., Bielski S., Novikova A., and Romaneckas K., 2019. Straw stocks as a source of renewable energy. A case study of a district in Poland. Sustainability, 11, 4714. https://doi.org/10.3390/su11174714.

Matysiak A., Wójtowicz A., and Oniszczuk T., 2018. Process efficiency and Energy consumption during the extrusion of potato multigrain formulations. Agric. Eng., 22, 2, 49-57. https://doi.org/10.1515/agriceng-2018-0015.

Mitrus M., Wójtowicz A., Kocira S., Kasprzycka A., Szparaga A., Oniszczuk T., Combrzyński M., Kupryaniuk K., and Matwijczuk A., 2020. Effect of extrusion-cooking conditions on the pasting properties of extruded white and red bean seeds. Int. Agrophys., 34(1), 25-32. https://doi.org/10.31545/intagr/116388.

Niedziółka I., Szpryngiel M., and Zaklika B., 2012. Analysis of physical and mechanical properties of pellets made of selected plant materials. Autobusy, 11, 79-86.

Ong H.C., Yu K.L., Chen W.H., Pillejera M.K., Bi X., Tran K.Q., and Pétrissans M., 2021. Variation of lignocellulosic biomass structure from torrefaction: A critical review. Renew. Sust. Energ. Rev., 152, 111698. https://doi.org/10.1016/j.rser.2021.111698.

Perea-Moreno M.A., Samerón-Manzano E., and Perea-Moreno A.J., 2019. Biomass as renewable energy: Worldwide research trends. Sustainability, 11, 863. https://doi.org/10.3390/su11030863.

Sadowska U., Matwijczuk A., Niemczynowicz A., Dróżdż T., and Żabiński A., 2019. Spectroscopic examination and chemometric analysis of essential oils obtained from peppermint herb (*Mentha piperita* L.) and caraway fruit (*Carum carvi* L.) subjected to pulsed electric fields. Processes, 7, 466. https://doi.org/10.3390/pr7070466.

Vandenbossche V., Brault J., Vilarem G., Hernández-Meléndez O., Vivaldo-Lima E., Hernández-Luna M., Barzana E., Duque A., Manzanares P., and Ballesteros M., 2014. A new lignocellulosic biomass deconstruction process combining thermo-mechano chemical action and biocatalytic enzymatic hydrolysis in a twin-screw extruder. Ind. Crops Prod., 55, 258-266. https://doi.org/10.1016/j.indcrop.2014.02.022.

Varma V.S., Das S., Sastri C.V., and Kalamdhad A.S., 2017. Microbial degradation of lignocellulosic fractions during drum composting of mixed organic waste. Sustain. Environ. Res., 27(6), 265-272. https://doi.org/10.1016/j.serj.2017.05.004.

Victorin M., Davidsson Å., and Wallberg O., 2020. Characterization of mechanically pretreated wheat straw for biogas production. Bioenergy. Res., 13, 833-844. https://doi.org/10.1007/s12155-020-10126-7.

Wang M., Wang J., Li Y., Li Q., Li P., Luo L., Zhen F., Zheng G., and Sun Y., 2022. Low-temperature pretreatment of biomass for enhancing biogas production: A Review. Fermentation, 8, 10, 562. https://doi.org/10.3390/fermentation8100562.

Xu J., Xu X., Liu Y., Li H., and Liu H., 2015. Effect of microbiological inoculants DN-1 on lignocellulose degradation during co-composting of cattle manure with rice straw monitored by FTIR and SEM. Environ. Prog. Sustain., 35(2), 345-351. https://doi:10.1002/ep.12222.

Zając T., Synowiec A., Oleksy A., Macuda J., Klimek-Kopyra A., and Borowiec F., 2017. Accumulation of biomass and bioenergy in culms of cereals as a factor of straw cutting height. Int. Agrophys., 31(2), 273-285. https:/doi:10.1515/intag-2016-0041.

Zhang L., Yang Z., Li S., Wang X., and Lin R., 2020. Comparative study on the two-step pyrolysis of different lignocellulosic biomass: Effects of components. JAAP, 152, 104966. https://doi.org/10.1016/j.jaap.2020.104966.

Zhang Y.Q., Fu E.H., and Liang J.H., 2008. Effect of ultrasonic waves on the saccharification processes of lignocellulose. Chem. Eng. Technol., 31(10), 1510-1515. https://doi.org/10.1002/ceat.200700407.

Zhang Y., Dian-Ming J., Zhen-lei X., Hao Z., Long-Hai L., Hai-Tao Ch., Shuang L., Rui L., and Sheng-Ming Z., 2021. Optimization of wheat straw pretreatment process parameters for straw mulch mat. BioResources, 16. 3827-3839. https://doi.org/10.15376/biores.16.2.3827-3839.

Zheng J. and Rehmann L., 2014. Extrusion pretreatment of lignocellulosic biomass: A review. Int. J. Mol. Sci., 15, 18967-18984. https://doi.org/10.3390/ijms151018967.

Zhuang J., Li M., Pu Y., Ragauskas A.J., and Yoo C.G., 2020. Observation of potential contaminants in processed biomass using fourier transform infrared spectroscopy. Appl. Sci., 10(12), 4345. https://doi.org/10.3390/app10124345.